THYROID
Volume 20, Number 11, 2010

DOI: 10.1089/thy.2009.0349

TSH Regulation Dynamics in Central and Extreme Primary Hypothyroidism

Marisa C. Eisenberg,[1,2] Ferruccio Santini,[3] Alessandro Marsili,[3]
Aldo Pinchera,[3] and Joseph J. DiStefano III[1]

Background: Thyrotropin (TSH) changes in extreme primary hypothyroidism include increased secretion, slowed degradation, and diminished or absent TSH circadian rhythms. Diminished rhythms are also observed in central hypothyroid patients and have been speculated to be a cause of central hypothyroidism. We examined whether TSH secretion saturation, previously suggested in extreme primary hypothyroidism, might explain diminished circadian rhythms in both disorders.
Methods: We augmented and extended the range of our published feedback control system model to reflect nonlinear changes in extreme primary hypothyroidism, including putative TSH secretion saturation, and quantified and validated it using multiple clinical datasets ranging from euthyroid to extreme hypothyroid (postthyroidectomy). We simulated central hypothyroidism by reducing overall TSH secretion and also simulated normal TSH secretion without circadian oscillation, maintaining plasma TSH at constant normal levels. We also utilized the validated model to explore thyroid hormone withdrawal protocols used to prepare remnant ablation in thyroid cancer patients postthyroidectomy.
Results: Both central and extreme primary hypothyroidism simulations yielded low thyroid hormone levels and reduced circadian rhythms, with simulated daytime TSH levels low-to-normal for central hypothyroidism and increased in primary hypothyroidism. Simulated plasma TSH showed a rapid rise immediately following triiodothyronine (T_3) withdrawal postthyroidectomy, compared with a slower rise after thyroxine withdrawal or postthyroidectomy without replacement.
Conclusions: Diminished circadian rhythms in central and extreme primary hypothyroidism can both be explained by pituitary TSH secretion reaching maximum capacity. In simulated remnant ablation protocols using the extended model, TSH shows a more rapid rise after T_3 withdrawal than after thyroxine withdrawal postthyroidectomy, supporting the use of replacement with T_3 prior to ^{131}I treatment.

Introduction

Two well-known hallmarks of normal thyrotropin (TSH) dynamics are high sensitivity to small changes in circulating thyroid hormone (TH) and circadian oscillations. TSH changes in extreme primary hypothyroidism include increased TSH secretion, slowed degradation (1), effects of compensatory changes in deiodinase activity, particularly type 2 deiodinase (D2) upregulation in brain (2–5), and diminished or absent circadian rhythms (6–8). Although the mechanism is unknown, diminished circadian rhythms also are observed in central hypothyroidism. Indeed, they are speculated to be one cause of the disease (6,7,9), although multiple factors may contribute to central hypothyroidism, including mutations in the thyrotropin releasing hormone (TRH) or TSH gene and improper glycosylation, among others (10–12).

We address these issues here by augmenting and extending a human TH feedback control system simulation model (13,14) into the extreme hypothyroid range, supported by human data in this range. We examine whether saturation of TSH secretion, previously suggested in extreme primary hypothyroidism (6), might explain diminished circadian rhythms in both disorders. We also explore potential effects of these putative changes in TSH secretion and elimination mechanisms on TH remnant ablation protocols used in thyroid cancer patients, again with the aid of the extended

[1]Biocybernetics Laboratory, Departments of Computer Science, Medicine, and Biomedical Engineering, University of California, Los Angeles, California.
[2]Mathematical Biosciences Institute, The Ohio State University, Columbus, Ohio.
[3]Department of Endocrinology and Metabolism, University of Pisa, Pisa, Italy.

simulator. After thyroidectomy for differentiated thyroid cancer, patients are typically given levothyroxine (L-T_4), L-triiodothyronine (T_3), or both, to reestablish the euthyroid condition, followed by withdrawal of TH,* to increase TSH levels prior to ^{131}I treatment to ablate any remnants or metastases (15–18). There remains some controversy concerning these protocols (15–18), so we simulated and compared them for their predicted rapidity in achieving targeted 30–50 mU/L TSH levels before ^{131}I treatment.

Methods

Brain submodel refinements in extreme primary hypothyroidism

The original model (13,14) (equations given in Appendix 1) was developed and quantified from human data reflecting mild to moderate hyper- and hypothyroid as well as normal states. It includes nonlinearities depicting enzymatic and protein-binding changes over the spectrum of normal and abnormal thyroid ranges. The brain submodels, however, were not developed for more extreme dynamic ranges. We augment and extend the model here to incorporate altered TSH dynamics in extreme hypothyroidism, including D2 upregulation and type 3 deiodinase (D3) downregulation in brain, nonlinear TSH degradation, and TSH saturation-based changes in circadian rhythms. Some model rate "constant" parameters have different values at the extremes of hormone level ranges. We represent these parameters over their entire dynamic range by defining nonlinear functions that match values at the extremes and transition smoothly between them. This approach maintains the form of the original model equations, with minimal additional model complexity, consistent with conventional receptor dynamical changes (e.g., receptor saturation) anticipated under abnormal conditions. We validate the expanded model in this broader range using additional clinical data.

Brain D2 upregulation. D2 expression in brain is upregulated in hypothyroidism (2,19,20). To accommodate this, we adjusted k_4, the constant rate parameter representing combined effects of plasma T_4 transport into brain and conversion to T_3 inside brain cells. With D2 upregulated, we expect k_4 to increase in hypothyroidism. We show in Appendix 2 that k_4 goes from $k_4 \approx k_3$ in euthyroids (where k_3 is the T_3 transport rate into the brain) to $k_4 \approx 6k_3$ in extreme hypothyroidism, based on data in rats and humans (3–5,21–25). To bridge these two ranges, we replaced the parameter k_4 with a smooth sigmoid transition function, designated $f_4(T_{3B})$ in Eq. [3] below, between the euthyroid/normal range of brain T_3 (denoted T_{3B}) and the extreme hypothyroid/thyroidectomized range. The relationship for f_4 varying with T_{3B} is derived in Appendix 2 and shown in Figure A2.

Brain D3 downregulation and TSH secretion. D3 is expressed in brain, with an inverse relationship between D3 activity and T_3 content demonstrated in various human cerebral regions (26). D3 is known to be downregulated in hypothyroidism, yielding slower brain T_3 degradation in extreme hypothyroidism (19). It has been also suggested that, in extreme hypothyroidism, the pool of TSH in the anterior pituitary available for secretion is drained more rapidly, so that TSH becomes less able to respond to rapid stimulation (3). The combined effects of both processes are represented as a "lag" in T_{3B} effects,† denoted $T_{3BLAG}(t)$, depicted in Eqs. [2] and [3] below. We quantified the lag time for this modified brain submodel in extreme hypothyroidism from human data in extreme hypothyroid patients (15), as described below.

Extreme-hypothyroid data. Hilts *et al.* (15) tested 13 patients 1–12 years after they were thyroidectomized and treated with ^{131}I for remnant ablation, following a T_3-only replacement protocol. Patients were switched from their usual T_4 replacement to 75–100 μg T_3 daily for 4 weeks, at which point T_3 therapy was discontinued. TSH was sampled over various intervals for each patient over the following 35 days, although sufficient samples for quantitative analysis were reported only for the first 15 days (15).

The new TSH secretion portion of the brain submodel, modified to include the above changes in D2 and D3, is given by the following three equations (Eq. [2] here is new):

$$SR_{TSH} = \left(B_0 + A_0 f_{CIRC} \sin\left(\frac{2\pi}{24}t - \phi_{phase}\right)\right) e^{-T_{3BLAG}} \quad [1]$$

$$\frac{dT_{3BLAG}}{dt} = f_{LAG}(T_{3B})\left(T_{3B} - T_{3BLAG}\right) \quad [2]$$

$$\frac{dT_{3B}}{dt} = \frac{f_4}{T_{4PEU}} T_{4P} + \frac{k_3}{T_{3PEU}} T_{3P} - k_{degT3B} T_{3B} \quad [3]$$

All variables SR_{TSH}, T_{3BLAG}, T_{4P}, T_{3B}, and T_{3P} are functions of time t, that is, $T_{3BLAG} \equiv T_{3BLAG}(t)$, etc. The new function f_{CIRC} in Eq. [1] represents alternative hypotheses about diminished circadian rhythms in extreme hypothyroidism. These are described in detail in the next section and Appendix 1. SR_{TSH} in Eq. [1] represents the secretion rate of TSH, including both basal and circadian components, damped by T_{3BLAG} T_{3BLAG} in Eqs. [1] and [2] is the lagged version of $T_{3B}(t)$, and f_{LAG} is the function controlling the lag time, with values dependent on $T_{3B}(t)$. We estimated the value of f_{LAG} in the extreme-hypothyroid range by optimally fitting it to the corresponding extreme-hypothyroid data (15) [using the program SAAM II (27), as in refs. (13,14)]. We assumed the fraction of normal TH secretion remaining after thyroidectomy and remnant ablation (15) to be zero. To support this assumption, we also tested a range of residual secretions fractions up to 1%, with no significant changes in results. To represent the transition from little to no lag in euthyroidism to significant lag in extreme hypothyroidism, we use a smooth nonlinear sigmoid function for f_{LAG} (T_{3B}) in Eq. [2], with details described in the Results section and Appendix 1.

Similarly, D2 effects on brain T_4-to-T_3 conversion in the extreme-hypothyroid range are represented by the coefficient

*Alternatively, dosing with recombinant-human TSH (rhTSH) may be used to increase TSH levels prior to ^{131}I treatment. This protocol is not addressed in this work.

†This is equivalent to a low-pass filter in engineering signal analysis, suppressing the higher-frequency components of the TSH signal.

$f_4 \equiv f_4(T_{3B})$ in the first term of Eq. [3], a sigmoidal function of T_{3B} derived in Appendix 2 and shown in Figure A2. This new function is used to shift smoothly between normal ($f_4 \approx k_3$) and extreme hypothyroid values ($f_4 \approx 6k_3$) of f_4.

Reduced TSH circadian rhythms: pituitary TSH saturation. TSH in normal human subjects shows a significant daily circadian rhythm, with a maximum near 2 a.m., and a daytime nadir. Normal circadian rhythm amplitude is $\geq$50% of daily mean TSH (7,28,29). In profound primary hypothyroidism, circadian rhythms are diminished (6–8), although the mechanistic cause remains speculative.

One possibility is that circadian rhythm magnitude saturates (reaches a maximum), whereas basal TSH secretion continues to increase as TH levels fall. Thus the relative magnitude of the circadian variation compared with mean daily TSH would diminish until it becomes difficult to detect circadian variation compared with the larger magnitude of basal TSH. We denote this hypothesis as the saturating circadian rhythm (SCR) model, shown in purple in Figure 1.

Alternatively, the magnitude of circadian oscillation may increase initially as TH levels fall (and basal TSH increases) in hypothyroidism and then fall with more extreme low TH values (high TSH values). A possible mechanism for explaining this phenomenon might be as follows. As TH levels fall, TSH secretion increases, until basal TSH secretion reaches maximum capacity, with all available TSH immediately secreted. Thus, signals to increase secretion for the nightly surge become ineffective, as TSH secretion is already saturated (has reached its maximum). This is supported by studies showing attenuation of the TSH response to TRH in hypothyroidism (30). This hypothesis is denoted the diminishing circadian rhythm (DCR) model, shown as dashed green curve in Figure 1. A similar hypothesis was suggested in ref. (6), with TSH circadian amplitude limited because the pituitary was "unable to increase the TSH production beyond its capacity."

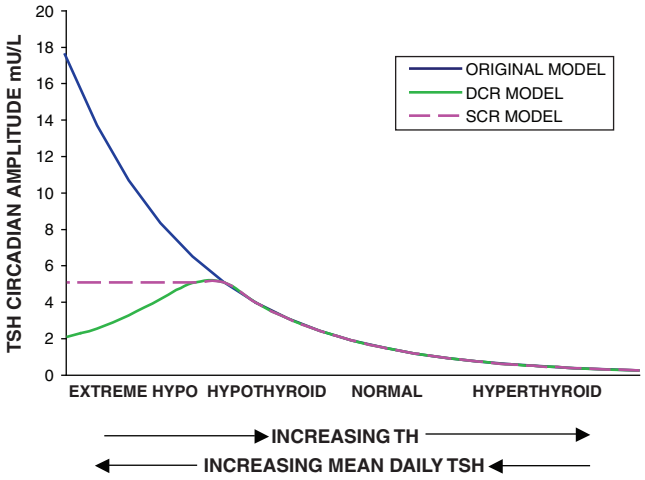

FIG. 1. Three possible relationships between brain triiodothyronine (T3) and thyrotropin (TSH). Blue: original simulation model in which TSH circadian rhythms grow as thyroid hormone (TH) falls. Purple dashes: SCR model—TSH circadian rhythms saturate as TH falls/mean plasma TSH increases. Green: diminishing circadian rhythm (DCR) model—TSH circadian rhythms saturate around and then fall as TH falls. *X*-axis arrows indicate direction of increasing hormone concentration. Color images available online at www.liebertonline.com/thy.

We define the TSH daily circadian range by the nighttime maximum TSH value minus the daytime nadir TSH value, and the TSH circadian rhythm amplitude by (daily circadian range)/2. We also use an alternative measure of circadian oscillation magnitude, average nighttime minus average daytime TSH, denoted the mean circadian difference (ΔTSH).

SCR model. To quantify the maximum TSH circadian amplitude (see purple curve in Fig. 1), we used two human clinical datasets. Weeke and Laurberg (8) studied six patients with severe hypothyroidism (basal TSH levels ranging from 35 to 96 mU/L), three with mild hypothyroidism, and five with treated severe hypothyroidism; Hirshberg *et al.* (7) studied 10 thyroidectomized patients preparing for radiotherapy, with basal TSH levels ranging from 42 to 156 mU/L. Hirshberg *et al.* measured a circadian range (max–min) of $\leq$10% of the daily mean/basal TSH level in extremely hypothyroid (thyroidectomized) patients. Average basal TSH among these 10 patients was 93.9 mU/L, suggesting a maximum TSH circadian range of $\sim$9.4 mU/L (daily fluctuation at most $\pm$4.7 mU/L about the basal value). This is consistent with Weeke and Laurberg's results, in which both severe and mildly hypothyroid patients stayed within this range and were also consistent with normal circadian amplitudes, typically $\sim$1–2 mU/L above/below the mean (daily circadian range of 2–4 mU/L). Based on these results, we implemented a maximum circadian amplitude of 5 mU/L, yielding a daily circadian range of 10 mU/L.

DCR model. This hypothesis is depicted by a green curve, which falls below the dashed purple curve in Figure 1. The literature is equivocal on the degree of circadian amplitude reduction. Some studies in hypothyroids report circadian rhythms in all patients (31), whereas others report mixed results, with some exhibiting no apparent rhythm (6–8). This suggests that the decrease shown in Figure 1 probably varies from patient to patient. We model only population average behavior, based on this clinical data. Additionally, the SCR model incorporates a maximum TSH amplitude based on the same clinical data (6–8) and acts as an upper bound for actual TSH circadian amplitude. Thus, alternative models of circadian rhythm decrease can be bounded by the SCR model.

Data for quantification. Adriaanse *et al.* (6) studied the difference between average day and nighttime TSH levels (mean circadian difference) in human subjects with varying degrees of hypothyroidism (Fig. 2). For normal controls they found mean TSH = 1.7 $\pm$ 0.7 (SD) mU/L with mean circadian difference of 1.0 $\pm$ 0.6 mU/L, and for subclinical hypothyroid patients, mean TSH = 10.5 $\pm$ 6.5 mU/L with mean circadian difference = 4.1 $\pm$ 2.5 mU/L (averages across 16 normals and 7 subclinical hypothyroids). Of the nine hypothyroid patients studied, only three demonstrated a detectable rhythm. Daily mean TSH among hypothyroids with detectable circadian rhythm was 73 $\pm$ 51 mU/L, and 266 $\pm$ 139 mU/L among patients with insignificant rhythm. The mean circadian difference for all nine hypothyroid patients was 3.9 $\pm$ 19 mU/L. Mean circadian differences for the two hypothyroid

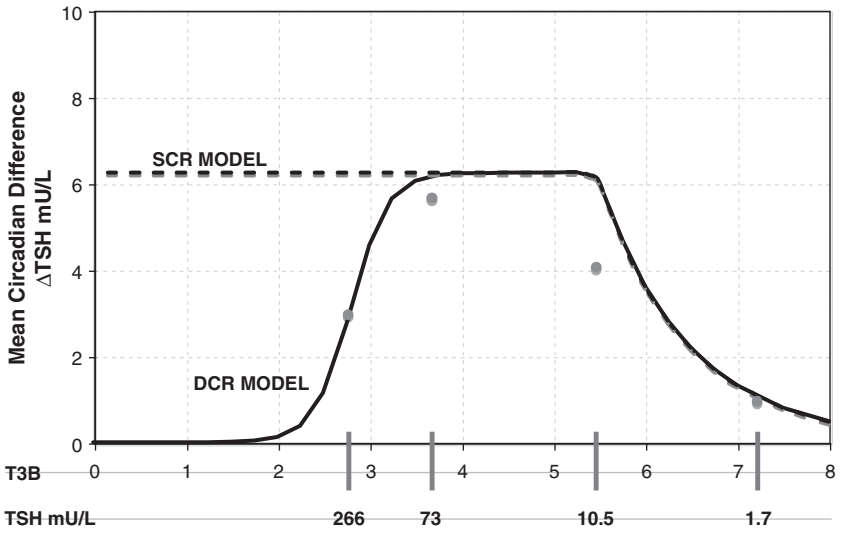

FIG. 2. Mean circadian difference as a function of T_{3B} and plasma TSH. Circles represent clinical data (6). Solid line represents simulations using the DCR and dashed line the SCR model. DCR circadian amplitude reaches a limit of zero in complete saturation.

subgroups were not reported. If the mean circadian difference among the six patients with undetectable rhythm was less than 3 mU/L, then mean circadian difference among the three patients with detectable circadian rhythm must be at least 5.7 mU/L.[‡]

Using the maximum TSH amplitude determined in the SCR model above, we chose a diminishing function of T_{3B}, which approximately matched the data shown in Figure 2, that is, saturating at a maximal circadian amplitude of 5 (7,8), then decreasing to a mean circadian difference of ~3 at 266 mU/L mean TSH. Derivations for the SCR and DCR models are given in Appendix 1.

TSH distribution and elimination. Under normal conditions, TSH disappearance from human plasma is well approximated as a single exponential with a half-life of ~55 minutes (1,14,32), yielding $k_{\mathrm{degTSH}}^{\mathrm{normal}} = 0.756\ \mathrm{hours}^{-1}$ (14). In extreme primary hypothyroid patients, TSH exhibits slowed degradation—likely due at least partly to increased sialylation (33–36)—with a longer, ~78 minutes, half-life (1), equivalent to $k_{\mathrm{degTSH}}^{\mathrm{hypo}} = 0.53\ \mathrm{hours}^{-1}$. To accommodate the changes smoothly, we represent the TSH degradation rate as a constant baseline degradation rate $k_{\mathrm{degTSH}}^{\mathrm{normal}} = 0.53\ \mathrm{hours}^{-1}$ plus a conventional Hill-type function of plasma TSH, together designated f_{degTSH} ($\mathrm{TSH_P}$).

$$f_{\mathrm{degTSH}}(\mathrm{TSH_P}) = 0.53 + \frac{V_{\mathrm{maxTSH}}}{K_{50}^{\mathrm{TSH}} + \mathrm{TSH_P}} \qquad [4]$$

The V_{maxTSH} and K_{50}^{TSH} (Table 1) were chosen to smoothly match an ~55 minutes half life in the normal range [0.5–5 mU/L TSH (37)] and 78 minutes in extreme hypothyroidism [~100 mU/L TSH (1)]. The dynamics of plasma $\mathrm{TSH_P}$ has the same form as in our earlier model, TSH secretion rate $\mathrm{SR_{TSH}}(t)$ balanced by degradation rate $f_{\mathrm{degTSH}}\mathrm{TSH_P}(t)$, with the exception that constant k_{degTSH} is replaced by variable f_{degTSH}, that is,

$$\frac{d\mathrm{TSH_P}}{dt} = \mathrm{SR_{TSH}} - f_{\mathrm{degTSH}}\mathrm{TSH_P} \qquad [5]$$

where we have abbreviated the function f_{degTSH} in [5] as $f_{\mathrm{degTSH}}(\mathrm{TSH_P}) \equiv f_{\mathrm{degTSH}}$.

Simulation studies

Euthyroid range model verification. The brain submodel extensions described above were incorporated into the hypothalamic–pituitary–thyroid (HPT) axis model (13,14), including effects of D2 upregulation, D3 downregulation, and changes in TSH kinetics (distribution and elimination submodel). We validated its fidelity with these updated components by comparing model simulations with normal plasma TSH, T_3, and T_4 data and the pharmacokinetic (PK) L-T_4 response study data used to quantify our original model (14,38).

Primary hypothyroidism. We simulated primary hypothyroidism, with TH secretion rates ranging from 50% down to 0.01% of normal.

Pisa protocol simulations: model validation and predictions. Thyroidectomy of patients with differentiated thyroid cancer is typically followed by oral TH treatment, withdrawal, and ^{131}I treatment to ablate thyroid remnants. A standard protocol is to withdraw normalizing oral L-T_4 given after surgery for 3–6 weeks, to raise TSH levels to 30–50 mU/L or higher, because residual thyroid remnants or metastases are best treated when TSH levels are high (17,18). Patients can be quite sick and impaired during withdrawal, because of the severe clinically hypothyroid condition generated. A variant protocol, with reportedly less morbidity, is used at the University of Pisa (17,18,39), illustrated in Figure 3.

Thyroidectomized patients scheduled for radionuclide imaging with ^{131}I are switched from L-T_4 to the shorter

[‡]If the mean circadian difference among the six patients was <3 mU/L, the sum of all six patients' mean circadian differences must be less than 6×3. As $\frac{(6\times3)+(3\times5.7)}{9} = 3.9$, the mean circadian difference among the remaining three patients must be at least 5.7 to yield an overall mean circadian difference of 3.9.

Table 1. Extended Brain Submodel Parameter Nomenclature, Estimates, Units, Variabilities, and Sources

Parameter	*Estimate*	*Units*	*%CV*[a]	*Definition and source*
A_0	581	μmol/h	61.4	TSH circadian rhythm amplitude constant, fitted to human data (34) in ref. (14)
A_{max}	2.37	μmol/h	—	Maximum TSH circadian rhythm amplitude, which yields a plasma TSH circadian amplitude of $\sim$5 mU/L, based on human data (7,8)
B_0	1166	μmol/h	60.7	TSH basal secretion constant, fitted to human data (34) in ref. (14)
F_3	0.0251	unitless	20.6	T_3 secretion fraction in the Pisa protocol, fitted to human data as described in the Methods section
F_4	0.0165	unitless	20.3	Thyroxine secretion fraction in the Pisa protocol, fitted to human data as described in the Methods section
k_3	0.118	hour^{-1}	6.43	Influx rate of plasma T_3 to TSH-regulatory brain areas, fitted to human data (34) in ref. (14)
F_4	0.118–0.708	hour^{-1}		Influx rate of plasma T_3 to TSH-regulatory brain areas; euthyroid value was fitted to human data (34) in ref. (14) and hypothyroid value was based on human and rat data (3–5,23–27)
$k_{deg T_{3B}}$	0.037	hour^{-1}	12.6	Degradation rate for T_{3B}, fitted to human data (34) in ref. (14)
k_{degTSH}^{hypo}	0.53	hour^{-1}	—	TSH degradation rate in extreme hypothyroidism, determined from human data (1,19)
f_{LAG}^{hypo}	0.0034	hour^{-1}	5.87	T_{3B} lag parameter, fitted to human data (15)
k_{50}^{TSH}	23	μmol	—	TSH distribution and elimination Hill-function parameter, based on human data (1,19)
ϕ_{phase}	-3.71	hour^{-1}	1.04	Phase constant such that TSH circadian rhythms peak at $\sim$2 a.m., fitted to human data (34) in ref. (14)
T_{3PEU}	0.006	μmol	—	T_{3B} normalization constant, determined by simulation in ref. (14)
T_{4PEU}	0.29	μmol	—	T_{3B} normalization constant, determined by simulation in ref. (14)
V_{maxTSH}	6.9	μmol/h	—	TSH distribution and elimination Hill-function parameter, based on human data (1,19)

[a]%CV = 100×SD/mean.
TSH, thyrotropin; T_3, triiodothyronine.

half-life hormone L-T_3[§] for replacement therapy. One week after L-T_4 cessation, patients are given 3 weeks of 20 μg T_3 twice daily. A 2-week wash-out period (no replacement therapy) normally follows T_3 treatment, immediately before ^{131}I administration. To examine T_3 dynamics under these conditions, a kinetic study was superimposed on this protocol, as shown in Figure 3, beginning 2 days before ^{131}I administration. Twenty patients were given an additional 20 μg T_3 in tablet form for 2 days before ^{131}I administration, with plasma T_3 and TSH measured over the subsequent 36 hours.

Using the new HPT axis model, we fitted the simulated T_3 and T_4 remnant fractions, F_3 and F_4, to this kinetic study data, that is, the fractions of normal T_3 and T_4 secretion rates (SR_3 and SR_4) remaining postthyroidectomy, expressed as $SR_3^{thyroX} = F_3 SR_3^{normal} = F_3 S_3 TSH_P(t-\tau)$ for T_3 and $SR_3^{thyroX} = F_4 SR_4^{normal} = F_4 S_4 TSH_P(t-\tau)$ for T_4. Both these equations are from Eq. 6 in ref. (13), where τ is the $\sim$7-hour mean secretion delay in response to TSH stimulation. Following quantification, we exercised the new simulation model to explore the predicted effects of the new brain submodel on replacement therapy and remnant ablation protocols.

Central hypothyroidism hypothesis testing. We simulated central hypothyroidism using both the updated model as well as the original HPT axis model (14), by setting overall TSH secretion rates to a range of values from 50% down to 0.01% of normal. To test the hypothesis that loss of circadian rhythmicity may cause hypothyroidism, we also simulated plasma TSH, T_3, and T_4 dynamics in response to a constant (nonoscillatory) TSH secretion rate, equal to the average rate of normal daily TSH secretion.

[§]T_3: Ti-Tre® 20 μg tablets (Teopharma, Italy).

Results

Brain submodel refinements

The new brain submodel equations and quantified parameters are given in Appendix 1 and Table 1, along with data sources. They extend the model domain and range to extreme hypothyroidism.**

Brain D3 downregulation and TSH secretion. The simulated TSH(t) response, using the extreme hypothyroid TSH secretion equations [1]–[4], is shown fitted to human data from Hilts *et al.* (15) in Figure 4. This yielded extreme hypothyroid $f_{LAG}^{hypo} = 0.0034$ hour^{-1} (Table 1), equivalent to a delay of $\sim$3 days between peak T_{3B} and peak T_{3BLAG}. For the normal T_{3B} range, we tested lags from 0 to 1 hour based on human data (40) and found no significant differences, so we chose $\sim$½ hour (Appendix 1). The continuous transition curve for f_{LAG} (Methods section and Appendix 1) smoothly merges the extreme hypothyroid range value for f_{LAG}^{hypo} with the normal range.

**The complete set of equations of the normal HPT axis model is given in ref. (14). To extend the range of the complete model, substitute the brain submodel equations in ref. (14) with the extended brain submodel equations given in Appendix 1.

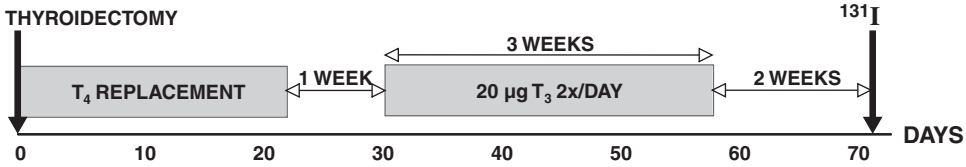

FIG. 3. Pisa protocol for remnant ablation following thyroidectomy for differentiated thyroid cancer. A T_3 kinetic study was superimposed on this protocol beginning on day 67.

Reduced TSH circadian rhythms in extreme hypothyroidism. Parameters and equations for the SCR and DCR models are given in Table 1 and Appendix 1. Figure 5 shows a comparison of the SCR, DCR, and original brain submodel simulations of TSH in primary hypothyroidism, with TH secretion set to 0.2% of normal.

Simulation studies

Model validation simulations with both SCR and DCR models were indistinguishable from our previous results in the euthyroid range (13,14). Euthyroid-range simulations of the PK L-T_4 response study also matched previous results (14,38).

Primary hypothyroidism. Simulated TSH dynamics in hypothyroidism postthyroidectomy is shown in graded fashion using the SCR model in Figure 6, with TH secretion rates (both SR_3 and SR_4) ranging from 100% down to 0.1% of normal. DCR model simulations were similar (not shown), but with somewhat further reduced circadian rhythms, for example, as in Figure 5.

Pisa protocol simulations. Our simulated results fit our human plasma T_3 kinetics data and (sparsely measured) TSH data values well, with patient data shown as circles and simulations shown as curves in Figure 7. Simulated plasma TSH(t) shows a rapid surge immediately following cessation of T_3 replacement. Fitted T_3 and T_4 remnant fractions were $F_3 = 0.0251$ and $F_4 = 0.0165$ (Table 1). Additional Pisa protocol simulations with varying remnant fractions and lag parameter f_{LAG} are shown in Figures 8 and 9, illustrating the interdependence of these two parameters.

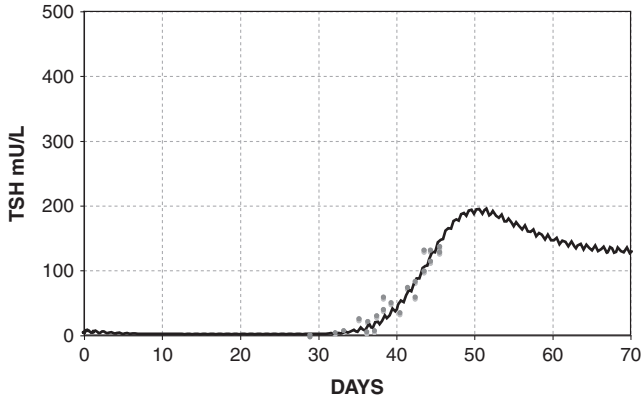

FIG. 4. Fit to human data by Hilts *et al.* (15), yielding extreme hypothyroid $f_{LAG}^{hypo} = 0.0034$ hour^{-1}, with the remnant fraction set to 0.5%. Data shown as circles, line represents the model simulation.

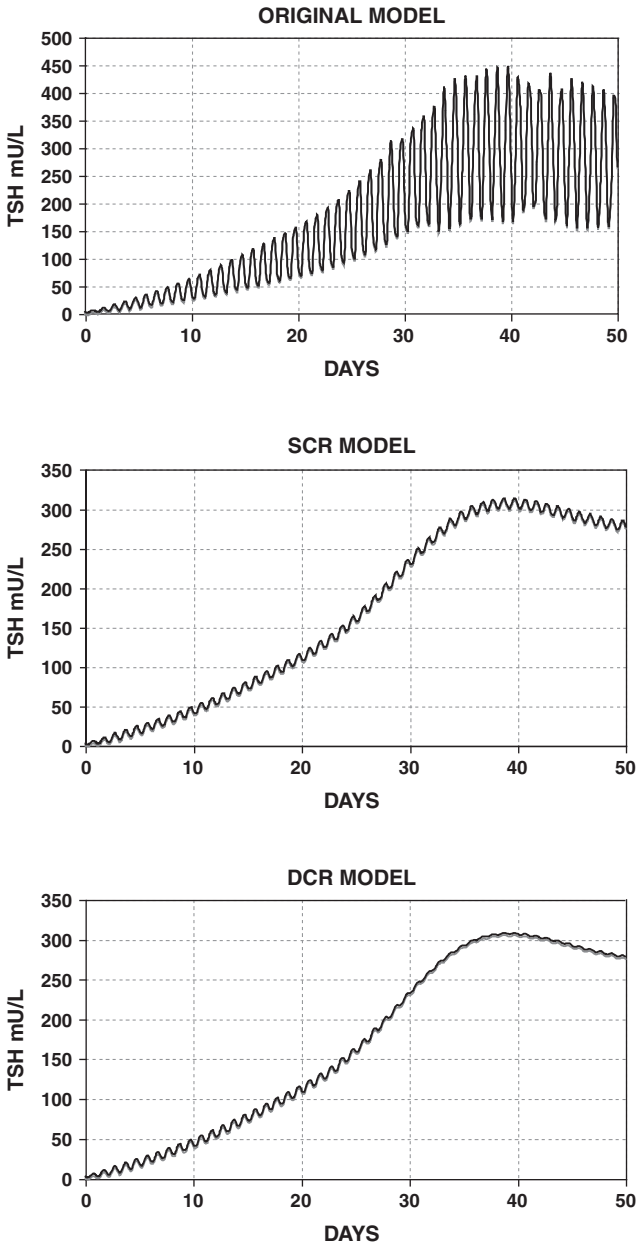

FIG. 5. Simulated extreme hypothyroidism postthyroidectomy with 0.2% remaining TH secretion using the original model (top) (14), and SCR (middle) and DCR (bottom) models extended to the extreme-hypothyroid range. Original model shows exaggerated circadian rhythms, whereas circadian variation in the new models is restricted to at most ~10 mU/L (SCR model) and further diminished with the DCR model.

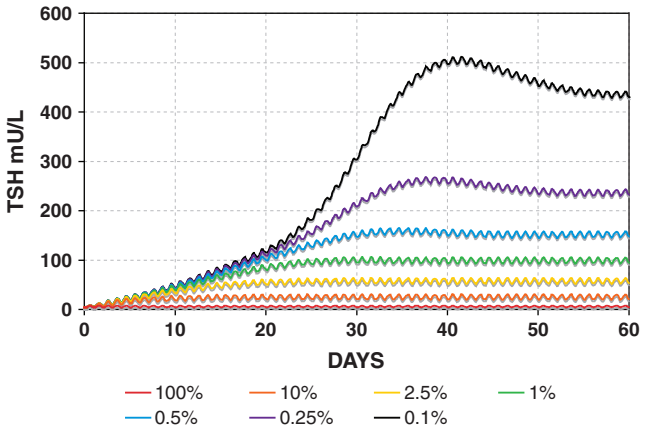

FIG. 6. Range of simulated primary hypothyroidism postthyroidectomy using the SCR model. TH secretion rates (SR_3 and SR_4) range from 100% (red) down to 0.1% of normal (black). Color images available online at www.liebertonline.com/thy.

Central hypothyroidism. SCR model results are shown in Figure 10. Results with the DCR model were similar (not shown). Note that both absolute TSH circadian amplitudes and relative TSH circadian amplitudes (circadian amplitude as a percentage of mean daily TSH) decrease with the degree of central hypothyroidism, eventually disappearing in most severe cases. In contrast, using the original brain submodel (14), relative TSH circadian amplitudes did not decrease, remaining ~50% of daily mean TSH for all levels. Using constant (nonoscillatory) normal mean daily TSH secretion, simulated plasma TSH, T_3, and T_4 reached constant, nonoscillatory, steady-state values in normal ranges: $TSH_P = 3.86\,mU/L$, $T_{3P} = 1.34\,ng/mL$, $T_{4P} = 6.68\,\mu g/dL$.

Discussion

Brain submodel extensions and new HPT axis model

We extended the functional range of the brain submodels to include extreme hypothyroid conditions. The changes were accomplished primarily by incorporating D2 upregulation and D3 downregulation in brain, nonlinear TSH degradation, and changes in TSH circadian rhythms resulting from pituitary TSH secretion saturation. Figure 4 and Appendix 1 illustrate a lag in TSH response to brain T_3 as hypothyroidism becomes more severe. The lag parameter k_{LAG} ($hour^{-1}$) represents brain D3 downregulation as well as potentially depleted pituitary TSH (6). We quantified the overall model with these changes using published data from human clinical data sources (with only one exception) (1,5,6,15,19,32). All model equations and parameter results are given in Appendix 1 and Table 1.

We implemented two alternative TSH secretion-saturation–based hypotheses, to account for attenuated circadian rhythms observed in extreme primary hypothyroidism, based on data ranging from euthyroid to extreme hypothyroid (6–8). The SCR and DCR hypothesis models (Figs. 1 and 2) were incorporated into the extended range HPT-axis model. Simulated circadian oscillation amplitudes in extreme hypothyroidism decreased significantly compared with oscillatory behavior of the original, limited-range model (Fig. 5) (14). The full extended-range model is now consistent with the clinical data (6–8).

We validated the extended-range HPT axis model using additional human data from the euthyroid to extreme hypothyroid ranges. Simulated mean euthyroid plasma T_3, T_4, and TSH levels as well as responses to L-T_4 dosing matched clinical data well (37,38) and were nearly identical to earlier euthyroid simulation results (14), confirming that the model extensions did not adversely affect performance in the euthyroid range.

We also validated the extended range of the model against independent data not used in its development. The data are from a PK study superimposed on a T_4-followed-by-T_3-replacement protocol (Fig. 3) in preparation for remnant ablation following thyroidectomy. Fitting T_3 and T_4 secretion fractions matched plasma T_3 and TSH data well (Fig. 7). The fitted T_3 secretion fraction was greater than the T_4 fraction ($F_3 = 0.0251$ vs. $F_4 = 0.0165$), both within reported remnant ranges postthyroidectomy (41). This is consistent with studies showing that T_3 is preferentially secreted in hypothyroidism (42,43).

Extreme primary hypothyroidism and replacement protocol simulations

For the $T_4 + T_3$ Pisa protocol (Figs. 3 and 7), simulated TSH increased rapidly after T_3 withdrawal. TSH rose more slowly for no replacement following thyroidectomy (Fig. 6) and also in a T_4-only withdrawal protocol (results not shown, similar to Fig. 6). For remnants up to 5% [range based on data in ref. (41)], we found that the simulated TSH response with no replacement reached 30 mU/L in ~1–2 weeks, consistent with earlier clinical observations (16,44–46).

Our results support the following hypothetical mechanism for this phenomenon, similar to that suggested in ref. (15). T_4 has an ~7-day half-life, so it lingers after thyroidectomy or after stopping L-T_4 replacement, slowing the rise of TSH. By contrast, a few weeks of T_3-only treatment, or T_3 after cessation of T_4 replacement (as in Fig. 3), allows remaining T_4 to be eliminated, while maintaining a relatively euthyroid state via T_3 dosing. When T_3 replacement is stopped, the remaining T_3 degrades quickly, causing TSH to rise rapidly as TH levels in brain fall.

The steepness of the simulated TSH rise after T_3 withdrawal was dependent on f_{LAG} (Fig. 8), the parameter representing effects of D3 downregulation, and secretion delays in the pituitary because of rapid draining of the intrapituitary TSH pool in times of high secretion. Hilts *et al.* (15) found that the rate of TSH rise after a similar T_3 withdrawal protocol varied from patient to patient (doubling times ranging from 1.5 to 3.6 days), suggesting that the extreme hypothyroid lag-time (f_{LAG}^{hypo}) may vary among patients. In addition, simulated steady-state TSH levels (Fig. 9) following the initial rise were dependent on the thyroid remnant fraction. The overall timing of peak TSH and the shape of the TSH rise following T_3 withdrawal appears to represent a balance of these two factors (among others), with larger remnant size delaying the peak time and larger f_{LAG}^{hypo} advancing it.

Hilts and others (15,17,18) have recommended using T_3-only replacement to achieve rapidly increased TSH levels postthyroidectomy, while minimizing hypothyroid symptoms. Recently, LeBoeuf and colleagues (16,47) challenged T_3 replacement protocols, suggesting that an L-T_4-only protocol

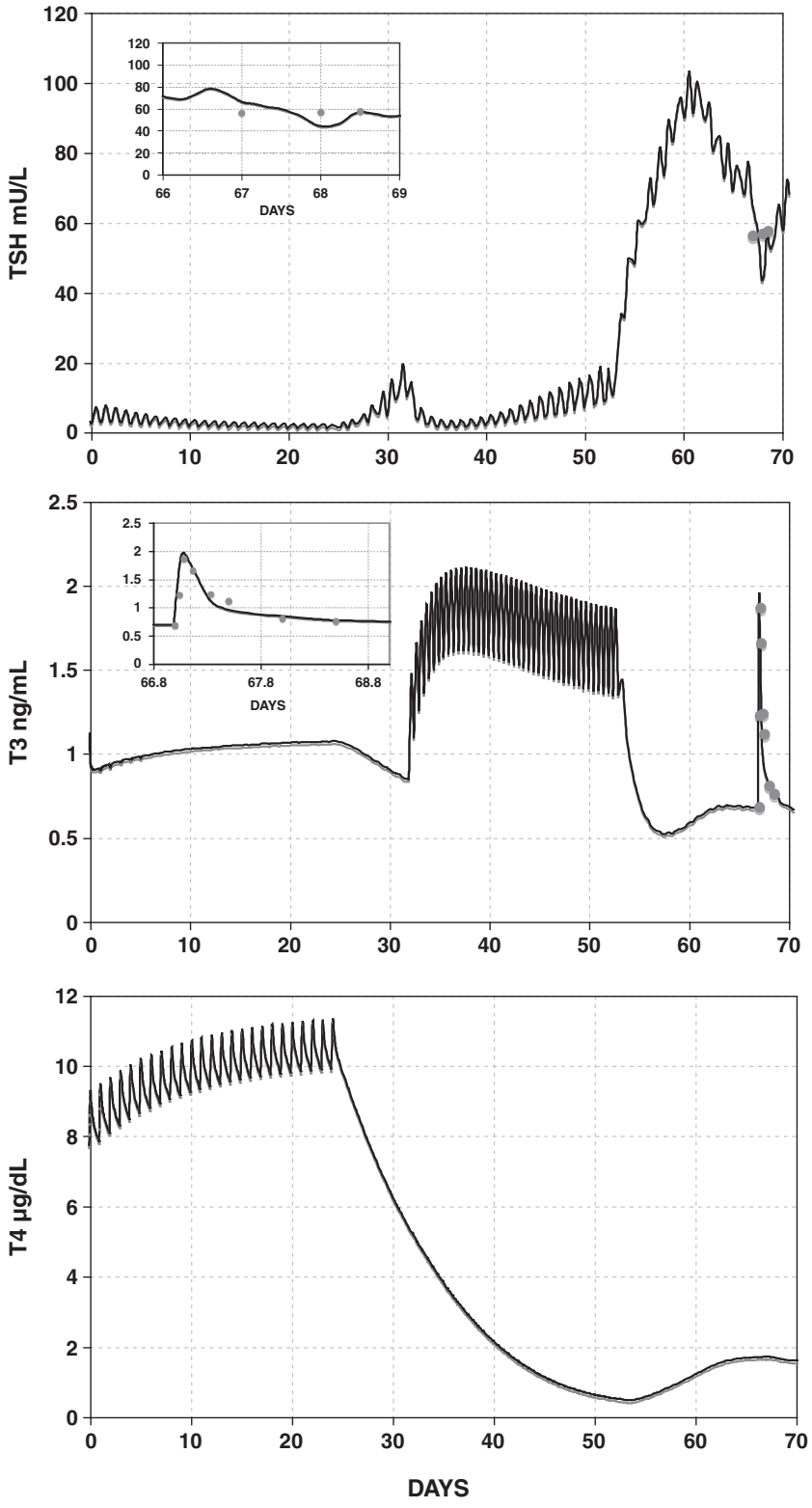

FIG. 7. Curves show simulated TSH(t), $T_3(t)$, and thyroxine(t) [$T_4(t)$] in the Pisa protocol using the SCR model, with individual remnant fractions fitted to the data, yielding $F_3 = 0.0251$ and $F_4 = 0.0165$. Patient data from kinetic study are shown as circles. Inset graphs show detail of simulation versus pharmacokinetic study data following an oral dose of 20 μg T_3 given on day 67. Remnant fraction is set to 0.02 (TH secretion rate is set to 2% of normal).

is adequate. They did observe similar rates of TSH increase following cessation of T_4 versus T_3 replacement—TSH reached 30 mU/L at 17 days after stopping T_4, and only 11 days after stopping T_3, compared with $\sim$10 days by the Hilts group (15). However, hypothyroid symptoms, as measured by Billewicz score, remained relatively unchanged for the first 2 weeks following an L-T_4-only withdrawal (16). These clinical data together with our simulation results suggest that while TSH rises more slowly after stopping L-T_4, remaining circulating T_4 may afford patients some respite from hypothyroid symptoms. Nonetheless, given the variable rates of rise seen in ref. (15) and in our simulations after T_3 withdrawal (Fig. 8),

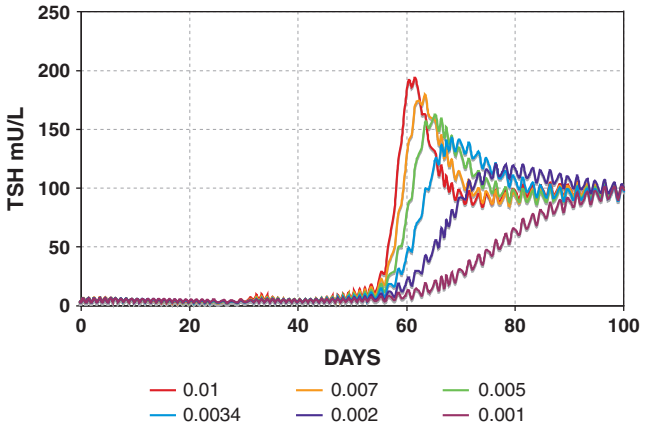

FIG. 8. Varying f_{LAG}^{hypo} determines the rate of simulated TSH rise following T_3 withdrawal in the Pisa protocol (Fig. 3). f_{LAG}^{hypo} is set to constant values ranging from 0.001 to 0.01 hour^{-1}; remnant fraction is set to 1%. Color images available online at www.liebertonline.com/thy.

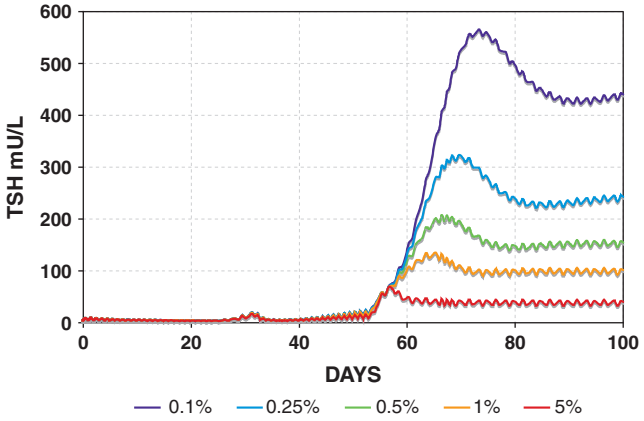

FIG. 9. Remnant fraction determines simulated steady-state TSH level in the Pisa protocol (Fig. 3). Remnant fractions are set from 0.1% to 5%. Color images available online at www.liebertonline.com/thy.

use of T_3 may still shorten the duration of hypothyroidism, at least for some patients. Indeed, T_3-only replacement prior to remnant ablation is becoming a more common practice in clinical settings (18,48).

Central hypothyroidism simulations

The SCR and DCR hypothesis models were designed specifically for attenuated circadian rhythms in primary hypothyroidism. Surprisingly, these refinements to the brain submodels also yielded decreased rhythms in central hypothyroidism simulations—an emergent property of the model. With the new HPT axis model, simulated steady-state TSH, T_4, and T_3 levels in simulated central hypothyroidism (Fig. 10) ranged from low to normal [normal ranges: 0.5–5 mU/L TSH, 5–12 μg/dL T_4, 0.8–1.9 ng/mL T_3 (37)]. These results match reports in the literature (9,49,50). Simulated TSH dropped rapidly at onset of reduced TSH secretion (Fig. 10, top right), followed by a slow rise to steady state (Fig. 10, top left). TSH circadian amplitude decreased significantly as TSH secretion was reduced for either SCR or DCR hypothesis implemented in the new simulator. Simulated TSH was roughly constant and likely undetectable for TSH secretion <5% of normal (Fig. 10, middle). By contrast, circadian amplitude with the original model without any adjustment for extreme primary hypothyroidism did not decrease, contrary to clinical data (7,9,50), remaining ~50% of mean TSH for all levels of central hypothyroidism.

Thus, our predictive model results support the hypothesis that reduced/absent circadian variation in extreme primary and central hypothyroidism may have the same underlying cause. Normally, as TSH secretion falls (Fig. 10, top right), decreasing TH stimulates the pituitary to increase TSH secretion. However, TSH secretion is impaired in central hypothyroidism, so maximum TSH secretion is lower than in euthyroids. As TSH reaches maximum secretory capacity, the pituitary may become unable to produce an additional nighttime surge, leading to diminished circadian rhythms (Fig. 10).

Alterations in TSH glycosylation and bioactivity also have been observed in both primary and central hypothyroidism (33–36,51–53). Higher sialylation of TSH resulting in lower intrinsic bioactivity of TSH may provide a mechanism contributing to TSH secretion saturation predicted by the model; alternatively, it may represent a compensatory effect of TSH secretion saturation, as highly sialylated TSH has a longer half-life (33,34), thereby extending its bioactive effects. The overall effects of TSH sialylation in humans are not entirely clear, as highly sialylated TSH has lower *in vitro* bioactivity but has been described to have higher *in vivo* bioactivity because of longer half-life (33,36).

It has been also suggested that decreased circadian rhythms may be a cause of central hypothyroidism (6,7,9). We tested this hypothesis by simulating normal TSH secretion without a circadian component, that is, constant TSH at the 24-hour mean value. Corresponding simulated T_3 and T_4 levels remained in the normal range, a result supported by evidence in humans with altered sleep schedules, yielding a loss of TSH rhythm, but normal plasma T_3 and T_4 levels (54). Thus, loss of rhythmicity alone is not likely sufficient to cause central hypothyroidism.

Conclusions

We extended and updated the HPT axis model for TH regulation to include mechanistically based regulatory changes in extreme hypothyroidism. These include slowed TH and TSH degradation, increased T_4-to-T_3 conversion, and diminished circadian rhythms. Simulation studies with the extended model support the hypothesis that diminished circadian rhythms in central and extreme primary hypothyroidism can both be explained by pituitary TSH secretion reaching maximal capacity. We also applied the new model to thyroid cancer. In simulated remnant ablation protocols using T_3 or T_4 or no-replacement therapy prior to ^{131}I treatment, TSH shows a more rapid rise after T_3 withdrawal than after T_4 withdrawal postthyroidectomy. This is due to residual T_4 slowing the rise of TSH. To reduce the time to achieve ~30 mU/L TSH levels, replacement with T_3 prior to ^{131}I treatment is suggested by these results.

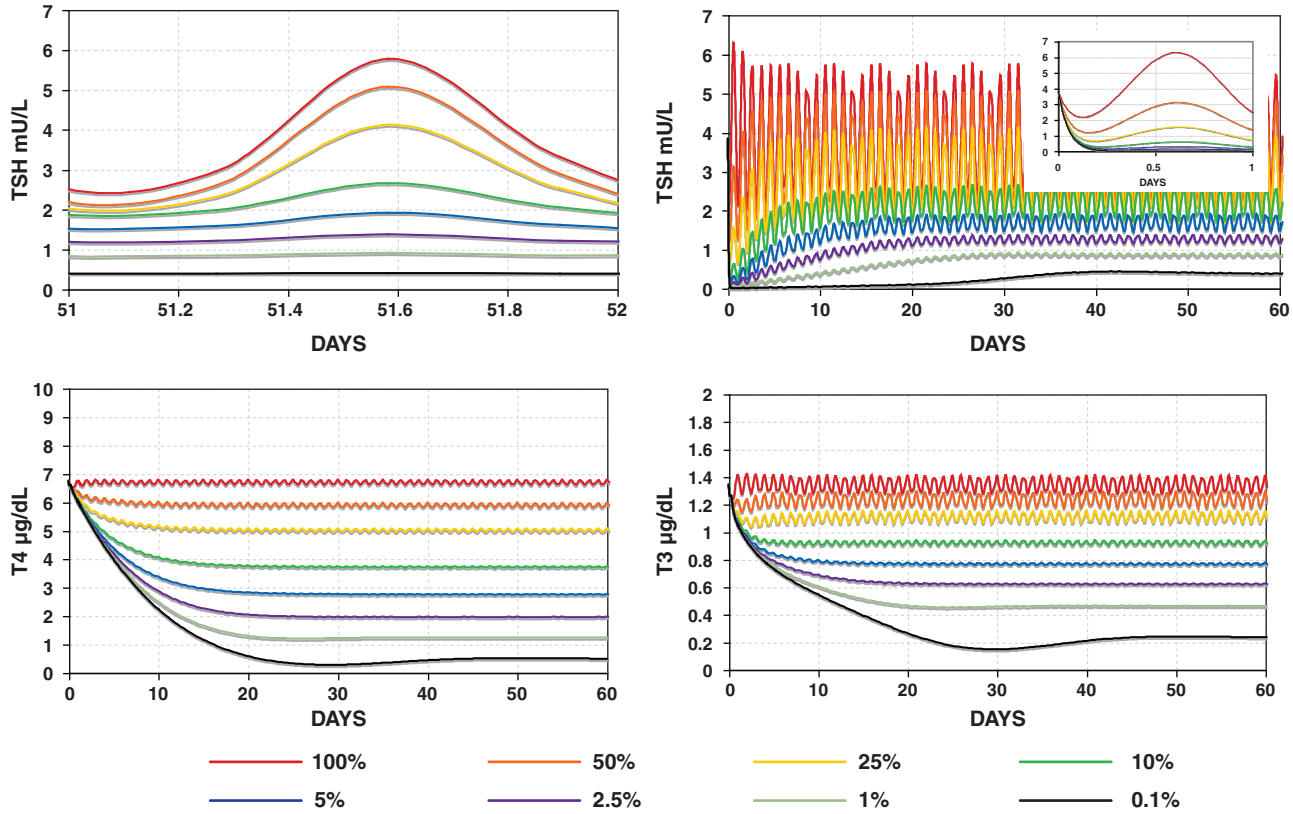

FIG. 10. Varying levels of central hypothyroidism (onset at $t = 0$) simulated using the SCR model with TSH secretion rates (SR_{TSH}) ranging from 100% down to 0.1% of normal. Top left: TSH circadian oscillation over 1 day in steady state. Top right: TSH in central hypothyroidism over 60 days. Inset graph: first day of simulated TSH, showing a rapid decline in TSH, followed by a slow rise to steady-state levels (shown top left). Bottom: T_3 and T_4 in central hypothyroidism over 60 days. Color images available online at www.liebertonline.com/thy.

Acknowledgments

The authors thank Dr. Reed Larsen (Harvard) for his helpful advice and insight regarding mechanisms of TSH secretion, and Dr. Mary Samuels (Oregon Health Sciences University) for providing us with circadian rhythm data and advice. This project was supported in part by a National Institutes of Health National Research Service Award (T32-GM008185) from the National Institute of General Medical Sciences, as well as the National Science Foundation under Agreement No. 0635561.

Disclosure Statement

The authors declare that no competing financial interests exist.

References

1. Ridgway EC, Weintraub BD, Maloof F 1974 Metabolic clearance and production rates of human thyrotropin. J Clin Invest **53:**895–903.
2. Guadano-Ferraz A, Escamez MJ, Rausell E, Bernal J 1999 Expression of type 2 iodothyronine deiodinase in hypothyroid rat brain indicates an important role of thyroid hormone in the development of specific primary sensory systems. J Neurosci **19:**3430–3439.
3. Larsen PR, Silva JE, Kaplan MM 1981 Relationships between circulating and intracellular thyroid hormones: physiological and clinical implications. Endocr Rev **2:**87–102.
4. Silva JE, Larsen PR 1978 Contributions of plasma triiodothyronine and local thyroxine monodeiodination to triiodothyronine to nuclear triiodothyronine receptor saturation in pituitary, liver, and kidney of hypothyroid rats. Further evidence relating saturation of pituitary nuclear triiodothyronine receptors and the acute inhibition of thyroid-stimulating hormone release. J Clin Invest **61:**1247–1259.
5. Silva JE, Larsen PR 1977 Pituitary nuclear 3,5,3′-triiodothyronine and thyrotropin secretion: an explanation for the effect of thyroxine. Science **198:**617–620.
6. Adriaanse R, Brabant G, Prank K, Endert E, Wiersinga WM 1992 Circadian changes in pulsatile TSH release in primary hypothyroidism. Clin Endocrinol **37:**504–510.
7. Hirshberg B, Veldhuis JD, Sarlis NJ 2000 Diurnal thyrotropin secretion in short-term profound primary hypothyroidism: Does it ever persist? Thyroid **10:**1101–1106.
8. Weeke J, Laurberg P 1976 Diurnal TSH variations in hypothyroidism. J Clin Endocrinol Metab **43:**32–37.
9. Caron PJ, Nieman LK, Rose SR, Nisula BC 1986 Deficient nocturnal surge of thyrotropin in central hypothyroidism. J Clin Endocrinol Metab **62:**960–964.
10. Collu R, Tang J, Castagne J, Lagace G, Masson N, Huot C, Deal C, Delvin E, Faccenda E, Eidne KA, Van Vliet G 1997 A novel mechanism for isolated central hypothyroidism: inactivating mutations in the thyrotropin-releasing hormone receptor gene. J Clin Endocrinol Metab **82:**1561–1565.
11. Faglia G, Bitensky L, Pinchera A, Ferrari C, Paracchi A, Beck-Peccoz P, Ambrosi B, Spada A 1979 Thyrotropin secretion in patients with central hypothyroidism: evidence for

reduced biological activity of immunoreactive thyrotropin. J Clin Endocrinol Metab **48:**989–998.
12. Sherman SI, Gopal J, Haugen BR, Chiu AC, Whaley K, Nowlakha P, Duvic M 1999 Central hypothyroidism associated with retinoid X receptor-selective ligands. New Engl J Med **340:**1075–1079.
13. Eisenberg M, Samuels M, DiStefano JJ 3rd 2006 L-T4 bioequivalence and hormone replacement studies via feedback control simulations. Thyroid **16:**1279–1292.
14. Eisenberg M, Samuels M, DiStefano JJ 3rd 2008 Extensions, validation, and clinical applications of a feedback control system simulator of the hypothalamo-pituitary-thyroid axis. Thyroid **18:**1071–1085.
15. Hilts SV, Hellman D, Anderson J, Woolfenden J, Van Antwerp J, Patton D 1979 Serial TSH determination after T3 withdrawal or thyroidectomy in the therapy of thyroid carcinoma. J Nucl Med **20:**928–932.
16. Leboeuf R, Perron P, Carpentier AC, Verreault J, Langlois MF 2007 L-T3 preparation for whole-body scintigraphy: a randomized-controlled trial. Clin Endocrinol **67:**839–844.
17. Pacini F, Molinaro E, Castagna MG, Lippi F, Ceccarelli C, Agate L, Elisei R, Pinchera A 2002 Ablation of thyroid residues with 30 mCi (131)I: a comparison in thyroid cancer patients prepared with recombinant human TSH or thyroid hormone withdrawal. J Clin Endocrinol Metab **87:**4063–4068.
18. Pacini F, Schlumberger M, Dralle H, Elisei R, Smit JW, Wiersinga W 2006 European consensus for the management of patients with differentiated thyroid carcinoma of the follicular epithelium. Eur J Endocrinol Eur Fed Endocr Soc **154:**787–803.
19. Bianco AC, Salvatore D, Gereben B, Berry MJ, Larsen PR 2002 Biochemistry, cellular and molecular biology, and physiological roles of the iodothyronine selenodeiodinases. Endocr Rev **23:**38–89.
20. Larsen PR 2009 Type 2 Iodothyronine deiodinase in human skeletal muscle: new insights into its physiological role and regulation. J Clin Endocrinol Metab **94:**1893–1895.
21. Patel YC, Burger HG 1973 Serum triiodothyronine in health and disease. Clin Endocrinol (Oxf) **2:**339–349.
22. Larsen PR, Dick TE, Markovitz BP, Kaplan MM, Gard TG 1979 Inhibition of intrapituitary thyroxine to 3,5,3′-triiodothyronine conversion prevents the acute suppression of thyrotropin release by thyroxine in hypothyroid rats. Journal of Clin Investig **64:**117–128.
23. Larsen PR, Frumess RD 1977 Comparison of biological effects of thyroxine and triiodothyronine in rat. Endocrinology **100:**980–988.
24. Patel YC, Pharoah PO, Hornabrook RW, Hetzel BS 1973 Serum triiodothyronine, thyroxine and thyroid-stimulating hormone in endemic goiter: a comparison of goitrous and nongoitrous subjects in New Guinea. J Clin Endocrinol Metab **37:**783–789.
25. Wennlund A 1986 Variation in serum levels of T3, T4, FT4 and TSH during thyroxine replacement therapy. Acta Endocrinol (Cph) **113:**47–49.
26. Santini F, Pinchera A, Ceccarini G, Castagna M, Rosellini V, Mammoli C, Montanelli L, Zucchi V, Chopra IJ, Chiovato L 2001 Evidence for a role of the type III-iodothyronine deiodinase in the regulation of 3,5,3′-triiodothyronine content in the human central nervous system. Eur J Endocrinol Eur Fed Endocr Soc **144:**577–583.
27. Barrett PH, Bell BM, Cobelli C, Golde H, Schumitzky A, Vicini P, Foster DM 1998 SAAM II: simulation, analysis, and modeling software for tracer and pharmacokinetic studies. Metab Clin Exp **47:**484–492.
28. Brabant G, Prank K, Ranft U, Schuermeyer T, Wagner TO, Hauser H, Kummer B, Feistner H, Hesch RD, von zur Muhlen A 1990 Physiological regulation of circadian and pulsatile thyrotropin secretion in normal man and woman. J Clin Endocrinol Metab **70:**403–409.
29. Weeke J 1973 Circadian variation of the serum thyrotropin level in normal subjects. Scand J Clin Lab Invest **31:**337–342.
30. Spencer CA, Schwarzbein D, Guttler RB, LoPresti JS, Nicoloff JT 1993 Thyrotropin (TSH)-releasing hormone stimulation test responses employing third and fourth generation TSH assays. J Clin Endocrinol Metab **76:**494–498.
31. Uberti ECD, Farah AH, Lovecchio G, Bagni B, Trasforini G, Margutti A, Alvisi V 1981 Circadian variations of plasma TSH in patients with severe hypothyroidism. Ric Clin Lab **11:**75–80.
32. Odell WD, Utiger RD, Wilber JF, Condliffe PG 1967 Estimation of the secretion rate of thyrotropin in man. J Clin Invest **46:**953–959.
33. Persani L 1998 Hypothalamic thyrotropin-releasing hormone and thyrotropin biological activity. Thyroid **8:**941–946.
34. Persani L, Borgato S, Romoli R, Asteria C, Pizzocaro A, Beck-Peccoz P 1998 Changes in the degree of sialylation of carbohydrate chains modify the biological properties of circulating thyrotropin isoforms in various physiological and pathological states. J Clin Endocrinol Metab **83:**2486–2492.
35. Persani L, Ferretti E, Borgato S, Faglia G, Beck-Peccoz P 2000 Circulating thyrotropin bioactivity in sporadic central hypothyroidism. J Clin Endocrinol Metab **85:**3631–3635.
36. Trojan J, Theodoropoulou M, Usadel KH, Stalla GK, Schaaf L 1998 Modulation of human thyrotropin oligosaccharide structures—enhanced proportion of sialylated and terminally galactosylated serum thyrotropin isoforms in subclinical and overt primary hypothyroidism. J Endocrinol **158:**359–365.
37. DeGroot LJ, Hennemann G 2010 Thyroid disease manager: the thyroid and its diseases. Available at www.thyroid manager.org/thyroidbook.htm, accessed September 2010.
38. Blakesley VA, Awni W, Locke C, Ludden TM, Granneman GR, Braverman LE 2004 Are bioequivalence studies of levothyroxine sodium formulations in euthyroid volunteers reliable? Thyroid **14:**191–200.
39. Marsili A, Santini F, Fierabracci P, Taddei D, Saponati G, Intrieri L, Pinchera A 2005 Kinetics, bioactivity and tolerability of 3,5,3′-triiodothyronine (T3) in an oral solution in thyroidectomized patients. J Endocrinol Investig **28:**356–357(suppl.).
40. Spencer CA, LoPresti JS, Nicoloff JT, Dlott R, Schwarzbein D 1995 Multiphasic thyrotropin responses to thyroid hormone administration in man. J Clin Endocrinol Metab **80:**854–859.
41. Lal G, Ituarte P, Kebebew E, Siperstein A, Duh QY, Clark OH 2005 Should total thyroidectomy become the preferred procedure for surgical management of Graves' disease? Thyroid **15:**569–574.
42. Faber J, Lumholtz IB, Kirkegaard C, Siersbaek-Nielsen K, Friis T 1982 Metabolic clearance and production rates of 3.3′-diiodothyronine, 3′,5′-diiodothyronine and 3′-monoiodothyronine in hyper- and hypothyroidism. Clin Endocrinol **16:**199–206.
43. Laurberg P 1984 Mechanisms governing the relative proportions of thyroxine and 3,5,3′-triiodothyronine in thyroid secretion. Metab Clin Exp **33:**379–392.
44. Grigsby PW, Siegel BA, Bekker S, Clutter WE, Moley JF 2004 Preparation of patients with thyroid cancer for 131I scintigraphy or therapy by 1–3 weeks of thyroxine discontinuation. J Nucl Med **45:**567–570.
45. Kuijt WJ, Huang SA 2005 Children with differentiated thyroid cancer achieve adequate hyperthyrotropinemia within

14 days of levothyroxine withdrawal. J Clin Endocrinol Metab **90:**6123–6125.
46. Serhal DI, Nasrallah MP, Arafah BM 2004 Rapid rise in serum thyrotropin concentrations after thyroidectomy or withdrawal of suppressive thyroxine therapy in preparation for radioactive iodine administration to patients with differentiated thyroid cancer. J Clin Endocrinol Metab **89:**3285–3289.
47. Leboeuf R, Perron P, Carpentier AC, Verreault J, Langlois MF 2008 There is no benefit of substitution of triiodothyronine for thyroxine in preparation of patients with thyroid carcinoma for further study or therapy. Clin Thyroidol **20:**9.
48. Cooper DS, Doherty GM, Haugen BR, Kloos RT, Lee SL, Mandel SJ, Mazzaferri EL, McIver B, Sherman SI, Tuttle RM 2006 Management guidelines for patients with thyroid nodules and differentiated thyroid cancer. Thyroid **16:**109–142.
49. McDermott MT, Ridgway EC 2001 Diagnosis and treatment of hypothyroidism. In: Cooper DS (ed) Medical Management of Thyroid Disease. Marcel Dekker, New York, pp 135–186.
50. Samuels MH, Lillehei K, Kleinschmidt-Demasters BK, Stears J, Ridgway EC 1990 Patterns of pulsatile pituitary glycoprotein secretion in central hypothyroidism and hypogonadism. J Clin Endocrinol Metab **70:**391–395.
51. Gyves PW, Gesundheit N, Thotakura NR, Stannard BS, DeCherney GS, Weintraub BD 1990 Changes in the sialylation and sulfation of secreted thyrotropin in congenital hypothyroidism. Proc Natl Acad Sci USA **87:**3792–3796.
52. Magner J 1990 Thyroid-stimulating hormone: biosynthesis, cell biology, and bioactivity. Endocr Rev **11:**354.
53. Magner J 1994 Biosynthesis, cell biology, and bioactivity of thyroid-stimulating hormone: update 1994. Endocr Rev Monogr **3:**55–60.
54. Brabant G, Prank K, Ranft U, Schuermeyer T, Wagner TOF, Hauser H, Kummer B, Feistner H, Hesch RD, Muhlen AV 1990 Physiological regulation of circadian and pulsatile thyrotropin secretion in normal man and woman. J Clin Endocrinol Metab **70:**403–409.

Address correspondence to:
Marisa C. Eisenberg, Ph.D.
Mathematical Biosciences Institute
The Ohio State University
378 Jennings Hall, 1735 Neil Ave.
Columbus, OH 43210
E-mail: meisenberg@mbi.osu.edu

Appendix 1. Original and Extended Brain Submodel Equations

Original Brain Submodel Equations (14)

$$\mathrm{SR_{TSH}}(t) = \left(B_0 + A_0 \sin\left(\frac{2\pi}{24}t - \phi_{\mathrm{phase}}\right)\right)e^{-T_{3B}(t)} \qquad [A1]$$

$$\frac{d\mathrm{TSH_P}(t)}{dt} = \mathrm{SR_{TSH}} - k_{\mathrm{degTSH}}\mathrm{TSH_P}(t) \qquad [A2]$$

$$\frac{dT_{3B}(t)}{dt} = \frac{k_4}{T_{4PEU}}T_{4P}(t) + \frac{k_3}{T_{3PEU}}T_{3P}(t) - k_{\mathrm{deg}T_{3B}}T_{3B}(t) \qquad [A3]$$

All rate (k) parameters are constant in Eqs. [A1]–[A3]. $\mathrm{SR_{TSH}}$ represents the thyrotropin (TSH) secretion rate by the anterior pituitary, $\mathrm{TSH_P}$ represents plasma TSH, and T_{3B} is a unitless, lumped variable representing triiodothyronine (T_3) in brain regions regulating TSH secretion. The first two terms in Eq. [A3] represent effects of plasma T_3 and thyroxine (T_4) on brain T_3, by transport into brain and $T_4 \rightarrow T_3$ conversion. Each term is normalized to euthyroid steady-state levels of T_3 and T_4 in plasma (T_{3PEU} and T_{4PEU}), both for dimensionality and to assist in deriving parameter constraints in ref. (14).

Extended Brain Submodel Equations

$$\mathrm{SR_{TSH}} = \left(B_0 + A_0 f_{\mathrm{CIRC}} \sin\left(\frac{2\pi}{24}t - \phi_{\mathrm{phase}}\right)\right)e^{-T_{3BLAG}} \qquad [1]$$

$$\frac{dT_{3BLAG}}{dt} = f_{\mathrm{LAG}}(T_{3B})\left(T_{3B} - T_{3BLAG}\right) \qquad [2]$$

$$\frac{dT_{3B}}{dt} = \frac{f_4}{T_{4PEU}}T_{4P} + \frac{k_3}{T_{3PEU}}T_{3P} - k_{\mathrm{deg}T_{3B}}T_{3B} \qquad [3]$$

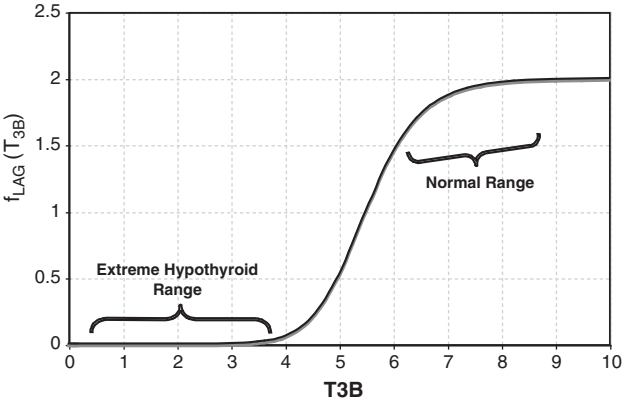

FIG. A1. $f_{\mathrm{LAG}}(T_{3B})$ as a function of T_{3B}. $f_{\mathrm{LAG}}^{\mathrm{hypo}} = 0.0034$ hour^{-1} (corresponding to a delay between peaks of $\sim$3 days) in the extreme-hypothyroid range and $\sim$2 hour^{-1} ($\sim$½ hour lag) in the normal range.

$$f_{\mathrm{degTSH}}(\mathrm{TSH_P}) = 0.53 + \frac{V_{\mathrm{maxTSH}}}{K_{50}^{\mathrm{TSH}} + \mathrm{TSH_P}} \qquad [4]$$

$$\frac{d\mathrm{TSH_P}(t)}{dt} = \mathrm{SR_{TSH}} - f_{\mathrm{deg\ TSH}}\mathrm{TSH_P}(t) \qquad [5]$$

Lagged brain T_3 in [1], that is, T_{3BLAG}, replaces T_{3B} in [A1]. In Eq. [2], the lagged T_{3B} function parameter $f_{\mathrm{LAG}}(T_{3B})$ (Fig. A1) is given as follows:

$$f_{\mathrm{LAG}}(T_{3B}) = k_{\mathrm{LAGhypo}} + \frac{2T_{3B}^{11}}{5.5^{11} + T_{3B}^{11}} \qquad [A4]$$

The second, Hill-function term is empirically derived to yield the curve shown in Figure A1. The parameter values for this function (namely 2, 5.5, and 11) are not meant to have biological significance, but are merely tuned such that f_{LAG} is near f_{LAG}^{hypo} in the extreme-hypothyroid range and equivalent to a delay of <1 hour in the normal range, based on human data (40).

In Eq. [3], f_4 replaces k_4 in [A3], with plasma T_4 effects on T_{3B} in the extreme-hypothyroid range represented as follows:

$$f_4 \equiv f_4(T_{3B}) = k_3 + \frac{5k_3}{1+e^{2T_{3B}-7}} \quad [A5]$$

f_4 versus T_{3B} is derived in Appendix 2 and shown in Figure A2. The second term in [A6] is a sigmoidal function of T_{3B} used to shift between normal and extreme-hypothyroid values of f_4 (from k_4), also derived in Appendix 2.

In Eq. [5], f_{degTSH} in [4] replaces $k_{degTSH}T_{3B}$ in [A2].

TSH secretion equations: defining f_{CIRC}

Saturating circadian rhythm (SCR) model: $f_{CIRC} = f_{SCR}$

$$SR_{TSH}(t) = \left(B_0 + A_0 f_{SCR} \sin\left(\frac{2\pi}{24}t - \phi_{phase}\right)\right) e^{-T_{3BLAG}(t)} \quad [A6]$$

The function $f_{SCR} \equiv 1 + \left(\frac{A_{max}}{A_0 e^{-T_{3BLAG}(t)}} - 1\right) \frac{1}{(1+e^{10T_{3BLAG}-55})}$ provides a cap for the TSH circadian amplitude, shown in Figures 1 and 2. The parameters were adjusted so that the amplitude of the TSH secretion oscillation, given by $A_0 f_{SCR} e^{-T_{3B}(t)}$, matches the original brain submodels (Eq. 1) in the normal range and saturates to a constant A_{max} in the extreme-hypothyroid range.

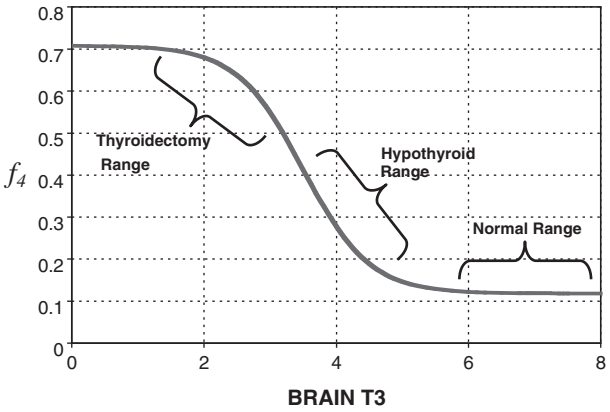

FIG. A2. Updated T_4 uptake and conversion parameter f_4 as a function of T_{3B} ranging from the normal [$f_4 = k_3 = 0.118$ (14)] to completely thyroidectomized ($f_4 = 6k_3 = 0.708$) range.

Diminishing circadian rhythm (DCR) model: $f_{CIRC} = f_{SCR} f_{DCR}$

$$SR_{TSH}(t) = \left(B_0 + A_0 f_{SCR} f_{DCR} \sin\left(\frac{2\pi}{24}t - \phi_{phase}\right)\right) e^{-T_{3BLAG}(t)} \quad [A7]$$

$f_{DCR} = \frac{1}{1+e^{-5T_{3BLAG}(t)+14}}$ is the diminishing function shown in Figure 2, which reduces TSH circadian rhythms to match clinical data (6) in the extreme-hypothyroid range.

Appendix 2. Type 2 Deiodinase–Upregulated k_4 Computations

The original brain submodel equations (14) are given in Eqs. [A1]–[A3].

We previously found $k_4 \approx k_3$ (14), based on available rat (3–5,22,23) and human (21,24,25) data. With type 2 deiodinase upregulated, we expect $k_4 > k_3$ in hypothyroidism. We derive an approximate relationship showing that type 2 deiodinase–upregulated k_4 is about six times greater than k_3 in extreme hypothyroidism, based on pituitary nuclear T3 data by Larsen and coworkers in thyroidectomized rats (4,5,22,23). Silva and Larsen (5) gave single intravenous (i.v.) injections (approximate impulses) of radiolabeled T_3 or T_4 to thyroidectomized rats and measured nuclear pituitary T_3 and plasma TSH. TSH response was strongly correlated with nuclear pituitary T_3, which suggests that nuclear pituitary T_3 dynamics may be approximately representative of our lumped variable T_{3B}. They also found that "800 ng T_4/100 g body weight (BW) gave the same degree of acute inhibition of TSH release, as rapidly as did 70 ng T_3/100 g" and yielded matching pituitary T_3 levels.

Suppose the same T_4/T_3 dose equivalence holds in humans (in our model equations above) and let T_{3B}^{800} be the T_{3B} response following 800 ng T_4, and T_{3B}^{70} the T_{3B} response following 70 ng T_3. Then these results collectively suggest that the T_{3B} responses to these two doses are approximately equal, that is, $T_{3B}^{800}(t) \approx T_{3B}^{70}(t)$, which implies $T_{3B}^{800}(t) \approx T_{3B}^{70}(t)$. Then, from Eq. 3, we have

$$k_4 \frac{T_{4P}^{800}(t)}{T_{4PEU}} + k_3 \frac{T_{3P}^{800}(t)}{T_{3PEU}} - k_{deg} T_{3B}^{800}(t) = k_4 \frac{T_{4P}^{70}(t)}{T_{4PEU}} + k_3 \frac{T_{3P}^{70}(t)}{T_{3PEU}} - k_{deg} T_{3B}^{70}(t)$$

where we let $T_{4P}^{800}(t)$ and $T_{3P}^{800}(t)$ be T_{4P} and T_{3P} following 800 ng T_4 (and similarly for $T_{4P}^{70}(t)$ and $T_{3P}^{70}(t)$). Canceling the $k_{deg}T_{3B}^{800}(t)$ and $k_{deg}T_{3B}^{70}(t)$ terms yields

$$k_4 \frac{T_{4P}^{800}(t)}{T_{4PEU}} + k_3 \frac{T_{3P}^{800}(t)}{T_{3PEU}} = k_4 \frac{T_{4P}^{70}(t)}{T_{4PEU}} + k_3 \frac{T_{3P}^{70}(t)}{T_{3PEU}}$$

$$\frac{k_4}{T_{4PEU}}(T_{4P}^{800}(t) - T_{4P}^{70}(t)) = \frac{k_3}{T_{3PEU}}(T_{3P}^{70}(t) - T_{3P}^{800}(t))$$

where the last equation is a rearrangement of the previous one.

If we let T_{4P}^{TX} and T_{3P}^{TX} represent steady-state plasma T_4 and T_3 levels postthyroidectomy, because of whatever thyroid remnants remain, and evaluate the above equation at $t = 0$ (approximating the i.v. bolus doses of 800 ng T_4/100 g BW and 70 ng T_3/100 g BW as impulses), we have

$$\frac{k_4}{T_{4PEU}}(T_{4P}^{800}(t) - T_{4P}^{70}(t))\,|_{t=0} = \frac{k_3}{T_{3PEU}}(T_{3P}^{70}(t) - T_{3P}^{800}(t))\,|_{t=0}$$

with

$$T_{4P}^{800}(t)\,|_{t=0} = \text{Dose}_4 + T_{4P}^{TX} \quad T_{3P}^{800}(t)\,|_{t=0} = T_{3P}^{TX}$$
$$T_{4P}^{70}(t)\,|_{t=0} = T_{4P}^{TX} \quad T_{3P}^{70}(t)\,|_{t=0} = \text{Dose}_3 + T_{3P}^{TX}$$

where Dose_4 and Dose_3 are the T_4 and T_3 doses. Substituting yields

$$\frac{k_4}{T_{4PEU}}(\text{Dose}_4 + T_{4PTX} - T_{4PTX}) = \frac{k_3}{T_{3PEU}}(\text{Dose}_3 + T_{3PTX} - T_{3PTX})$$
$$\frac{k_4}{T_{4PEU}}\text{Dose}_4 = \frac{k_3}{T_{3PEU}}\text{Dose}_3$$

Substituting for the dose and euthyroid steady-state plasma hormone levels $T_{4PEU} = 0.2978\,\mu$mol and $T_{3PEU} = 0.005158\,\mu$mol, we have

$$\frac{k_4}{T_{4PEU}}\frac{800\text{ ng } T_4}{100\text{ g BW}}\frac{1\text{ nmol } T_4}{777\text{ ng } T_4}\frac{1\ \mu\text{mol}}{1000\text{ nmol}} = \frac{k_3}{T_{3PEU}}\frac{70\text{ ng } T_3}{100\text{ g BW}}\frac{1\text{ nmol } T_3}{651\text{ ng } T_3}\frac{1\ \mu\text{mol}}{1000\text{ nmol}}$$

$$k_4 = k_3\frac{T_{4PEU}}{T_{3PEU}}\frac{70\text{ ng } T_3}{800\text{ ng } T_4}\frac{777\text{ ng } T_4/\text{nmol } T_4}{651\text{ ng } T_3/\text{nmol } T_3}$$

$$k_4 = k_3\ 57.73\frac{70\text{ ng } T_3}{800\text{ ng } T_4}\frac{777\text{ ng } T_4/\text{nmol } T_4}{651\text{ ng } T_3/\text{nmol } T_3}$$
$$k_4 = 6.03\ k_3 \approx 6\ k_3$$

Smooth transition from euthyroid k_4 to extreme hypothyroid k_4 via f_4

We used the sigmoid function $1/(1+e^{2T_{3B}-7})$ shown below to smoothly shift from $k_4 \approx k_3$ to $k_4 \approx 6k_3$ as T_{3B} levels shift from normal to thyroidectomized, yielding the following updated equations for k_4, now as a function of T_{3B} at time t:

$$f_4(T_{3B}) = k_3 + 5k_3/(1+e^{2T_{3B}-7})$$

which add an additional $5k_3$ to k_4 when in the extreme-hypothyroid/thyroidectomized range (so that in the extreme-hypothyroid range, $k_4 = k_3 + 5k_3 = 6k_3$). The parameter values for $f_4(T_{3B})$ (namely 2 and 7) are not meant to have biological significance, but are merely tuned such that the second term in $f_4(T_{3B})$ is negligible in the normal range of T_{3B} and $5k_3$ in the hypothyroid range. The overall behavior of f_4 as a function of T_{3B} is shown in Figure A2.